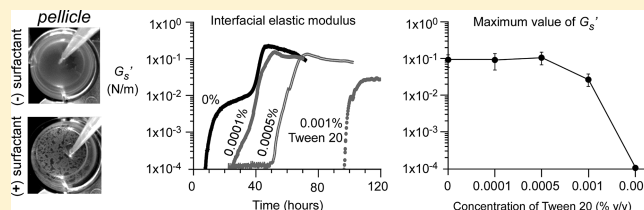


Disruption of *Escherichia coli* Amyloid-Integrated Biofilm Formation at the Air–Liquid Interface by a Polysorbate Surfactant

Cynthia Wu,^{†,§} Ji Youn Lim,^{‡,§} Gerald G. Fuller,^{*,†} and Lynette Cegelski^{*,‡}

[†]Department of Chemical Engineering and [‡]Department of Chemistry, Stanford University, Stanford, California 94305, United States

ABSTRACT: Functional amyloid fibers termed curli contribute to bacterial adhesion and biofilm formation in *Escherichia coli*. We discovered that the nonionic surfactant Tween 20 inhibits biofilm formation by uropathogenic *E. coli* at the air–liquid interface, referred to as pellicle formation, and at the solid–liquid interface. At Tween 20 concentrations near and above the critical micelle concentration, the interfacial viscoelastic modulus is reduced to zero as cellular aggregates at the air–liquid interface are locally disconnected and eventually eliminated. Tween 20 does not inhibit the production of curli but prevents curli-integrated film formation. Our results support a model in which the hydrophobic curli fibers associated with bacteria near the air–liquid interface require access to the gas phase to form strong physical entanglements and to form a network that can support shear stress.



INTRODUCTION

Bacterial biofilms are multicellular communities characterized by a complex extracellular polymeric matrix that surrounds the bacteria and promotes community cohesion, attachment to biotic and abiotic surfaces, and persistence in the environment and in the host.^{1,2} Most serious and persistent infectious diseases are biofilm-associated and are difficult and sometimes impossible to treat successfully as biofilm bacteria exhibit reduced sensitivity to host defenses and antibiotic treatment. Biofilms can also be detrimental in industrial settings and promote the contamination of surfaces and liquids in food and pharmaceutical industries. Undesired biofilms form in drinking water, in oil pipelines, and on the hulls of ships, leading to biofouling and biocorrosion.³ As we have become increasingly aware of the prevalence and importance of biofilm formation, particularly in the last 10 years, the number of studies on biofilm-integrated bacteria, in contrast to their planktonic and free-swimming counterparts, has also increased. Although biofilm formation is complex, due to the heterogeneity and insolubility of the extracellular polymeric matrix produced by the biofilm inhabitants, multiple laboratory models exist for studying biofilms in a reproducible manner, and it is clear that different growth, nutrient, and environmental conditions influence gene expression and the nature of biofilms, even when formed by the same bacterial species. The primary laboratory models include examining biofilm formation on agar, on abiotic surfaces such as plastic or stainless steel, and at the air–liquid interface. High-throughput analyses are possible when studying biofilm formation attached to plastic, due to convenient 96-well plate assays in which the biomass attached to plastic wells produced by biofilm formers can be quantified after staining with a dye such as crystal violet, and are routinely employed in biofilm inhibition studies.⁴ There are comparatively fewer studies on biofilms formed at an air–liquid interface, also referred to as pellicles.

We have been examining the contributions of bacterial amyloid fibers, termed curli, to biofilm formation by *Escherichia coli*. Curli are under study for their role in the pathogenesis of urinary tract infection and are commonly expressed by uropathogenic *E. coli* (UPEC) (including the one used in this study, UTI89). In addition, curli adhere to plants and to abiotic surfaces such as plastic and stainless steel and are commonly expressed by enterohemorrhagic *E. coli* isolates associated with food contamination and food-borne illness, such as the *E. coli* strain O157:H7.^{5–7} Curli are one of the most well-studied bacterial amyloids and are considered functional amyloids because the fibers contribute to the physiology and community behavior of *E. coli*.⁸ Bacteria also harness specific genetic and molecular machinery to direct the assembly of curli at the cell surface. Specifically, curli biogenesis requires nucleation-precipitation protein machinery encoded by the *csgBA* and *csgDEFG* operons.⁹ In vivo polymerization of the major curli subunit CsgA into β -sheet-rich amyloid fibers requires the nucleator protein, CsgB.¹⁰ CsgG is a membrane protein and CsgE and CsgF are assembly factors required for the stabilization and transport of CsgA and CsgB to the cell surface.^{11,12} Thus, *E. coli* regulate the production of amyloid fibers at the right time and the right place to influence adhesion and biofilm formation capabilities. Although curli was the first example of a bacterial amyloid to be described as amyloid in 2002,⁹ there has been an increasing number of bacterial amyloids discovered and characterized in the intervening ten years.^{5,6,13–17} The assembly of functional amyloids highlights the ability of Nature to harness the amyloid folding pathway for function in contrast to the well-recognized protein misassembly events that lead to aberrant protein oligomerization

Received: November 27, 2012

Revised: December 19, 2012

Published: December 21, 2012

and amyloid fiber formation of important eukaryotic amyloidogenic proteins such as amyloid β and α -synuclein associated with Alzheimer's and Parkinson's diseases, respectively. In the last several years, there is a growing awareness that such functional amyloids, not just in *Salmonella* and *E. coli*, but also in other microorganisms, share commonality in their ascribed functions and contribute to cellular physiology, adhesion, and biofilm formation.^{13–16} Thus, there is increased interest in learning how the integration of amyloids in biofilms influences the physical and chemical properties of the biofilm and how this impacts function and community behavior.

To better understand the mechanical and physicochemical features of amyloid-integrated pellicle formation by UPEC, we recently developed an integrated approach in order to correlate the molecular composition with the mechanical and interfacial rheological properties as a biofilm forms over time.¹⁸ We employed interfacial rheometry, commonly used to study complex fluids at interfaces, using a double wall ring interfacial rheometer. Imaging of the biofilm microstructure was accomplished using a Brewster angle microscope. This combination of methods monitored the mechanical and microstructural evolution of film formation in real time at the air–liquid interface. We used traditional biochemistry assays to quantify the production of amyloid proteins and to characterize cell growth and morphology. Using our physical-biochemical approach, we identified distinct temporal stages involved in pellicle formation that are associated with sensitive rheological signatures measured in real time (an increase in G' , the viscoelastic modulus, and aggregate detection by Brewster angle microscopy). The interfacial viscoelasticity of biofilm-forming bacteria exhibits a first phase in which bacteria grow at the air–liquid interface that is predominantly viscous, followed by a second phase during which the surface viscoelasticity increases as the biofilm forms. We also used our methodology to compare a typical biofilm with one formed under conditions that upregulate amyloid production (addition of moderate concentrations of DMSO or ethanol).⁴ The increased amyloid content accelerated the temporal onset of pellicle formation, increased the overall strength of the pellicle, and increased the ability of the biofilm to recover from mechanical strain, emphasizing the functional role that curli play in pellicle formation.

In contrast to the conditions described above where biofilm formation was enhanced, it is of greater interest, from a biofilm eradication standpoint, to identify strategies to prevent biofilm formation or disassemble existing biofilms. We hypothesized that a surfactant might prevent bacterial aggregation at the air–liquid interface and inhibit pellicle formation by UPEC. The interaction between surfactants and proteins has been extensively examined in the pharmaceutical industry where surfactants are used to solubilize and stabilize proteins and prevent antibody aggregation and denaturation,^{19–23} and in the food and the cosmetics industries where they are used to stabilize emulsions and foams.^{24–28} In addition, surfactants have been found to inhibit biofilm formation among some microorganisms including *Pseudomonas aeruginosa* and *Salmonella typhimurium*.^{29,30} Interestingly, in other bacteria, such as *Bacillus subtilis* and *Staphylococcus epidermis*, surfactants promote biofilm and pellicle formation, and, in some cases, these organisms produce their own surfactant.^{31–33} *B. subtilis*, for example, produces the lipopeptide surfactin, which triggers events that lead to enhanced community behavior and biofilm formation.³³ Thus, it is not immediately obvious whether a

surfactant should inhibit or promote bacterial biofilm formation. In this work, we present our discovery and experimental characterization of the inhibition of UPEC pellicle formation by the nonionic surfactant Tween 20.

MATERIALS AND METHODS

Bacterial Growth Conditions and Growth Assays. In all experiments, the UPEC isolate UTI89 and its curli mutant, UTI89 Δ csgA, were grown in YESCA (10g/L casamino acids, 0.5g/L yeast extract) nutrient medium. To investigate the influence of Tween 20 on bacterial growth, UTI89 were grown in 4 mL of YESCA broth containing various Tween 20 concentrations in 15 mL culture tubes with 200 rpm shaking at 26 °C. The 4 mL cultures were inoculated with 4 μ L of an overnight starter culture. Comparative growth curves of planktonic cells were obtained by measuring the cell culture optical density at 600 nm as a function of time. Total bacterial cell numbers (cfu/mL) were also enumerated after 24 h.³⁴

Surface Tensiometry. The surface tension of Tween 20 in deionized Millipore water and in YESCA medium was measured by the Wilhelmy plate method.³⁵ The balance was precalibrated and its accuracy was tested with deionized Millipore water to ensure the measured surface tension to be 72.7 ± 0.5 mN/m at room temperature. Specified amounts of Tween 20 were added to each solution to prepare 0.0001%–0.1% v/v final solutions in a 50 mL conical tube. Immediately after mixing, 20 mL of the solution was transferred to a sterilized beaker. The Wilhelmy plate was dipped into the solution, and the surface tension was measured over time. The equilibrium surface tension was recorded when no further changes in the value were observed.

Pellicle Assay. To evaluate the influence of Tween 20 on UTI89 pellicle formation, bacteria were grown in a 24-well plate at 26 °C with and without Tween 20. Pellicle formation was inspected visually and assessed by perturbation with a pipet tip after 5 days of incubation.

Crystal-Violet Staining Assay. A crystal-violet staining assay was used to examine UTI89 adhesion to plastic (PVC).³⁶ Briefly, bacterial cells were grown in 96-well PVC plates; unattached cells were removed through washes with phosphate-buffered saline (PBS), and the remaining adherent cells were stained with 0.1% crystal violet. The extent of biofilm formation was quantified by measuring the absorbance of crystal violet at OD₅₉₅ after dissolving the PVC-associated biomass in 95% ethanol.

Western Blot Assay. UTI89 whole cell samples were harvested after 18 and 48 h incubation at 26 °C in 4 mL of YESCA broth with various concentrations of Tween 20 in 15 mL culture tubes. Whole-cell samples with equivalent cell numbers were prepared as cell pellets of 1 mL of cell culture with an optical density at 600 nm (OD₆₀₀) of 1.0. Each pellet was treated with 100 μ L of hexafluoroisopropanol (HFIP) to dissociate curli subunits.³⁶ HFIP was removed by vacuum centrifugation, and samples were resuspended in sodium dodecyl sulfate polyacrylamide gel electrophoresis (SDS-PAGE) loading buffer. Protein gel electrophoresis was carried out using 12% SDS-PAGE gels (Invitrogen) and blotted onto 0.2 μ m pore size nitrocellulose transfer membranes (Whatman). The polyclonal rabbit antiserum to CsgA was used as the primary antibody, and horseradish peroxidase (HRP)-conjugated goat anti-rabbit antibody (Pierce) was used as the secondary antibody.³⁷

Transmission Electron Microscopy. Transmission electron microscopy (TEM) was used to visualize UTI89 curli expression. Bacteria were pelleted, washed, resuspended in PBS, and applied directly onto 300 mesh copper grids coated with Formvar film (Electron Microscopy Sciences, Hatfield, PA) for 2 min. Each grid was washed five times with deionized water and negatively stained with 2% uranyl acetate for 90 s. After 5 min of drying, electron microscopy was performed using a Jeol 1230 TEM instrument.

Interfacial Shear Rheometry. The viscoelastic dynamics of the surface was measured using an AR-G2 rheometer (TA Instruments) with a Du Noüy ring and a double-wall Couette Teflon flow cell apparatus as described previously.¹⁸ Briefly, the overnight culture of bacteria was diluted to 1:1000 with fresh YESCA broth containing the

appropriate concentration of Tween 20 (0.0001–0.1%, v/v) and then added to the Teflon flow cell apparatus. Evaporation loss during the experiments was compensated for by introducing fresh media to the subphase of the flow cell via a syringe. The Du Noüy ring was located at the culture/air interface and was set to oscillate at an angular frequency of 0.5 rad/s and a strain of 1% about its circular axis for up to 120 h. The instrument then reports the interfacial elastic modulus, $G_s'(\omega)$, and the interfacial viscous modulus, $G_s''(\omega)$. Afterward, a strain sweep from 0.001% to 100% at 0.5 rad/s angular frequency was performed to characterize the linear and the breakdown regions of the surface.

RESULTS AND DISCUSSION

Surface Activity of YESCA Medium and the Influence of Tween 20. In our studies, we examined biofilm formation in YESCA medium as a function of increasing Tween 20 concentration. We first examined the surface activities of Tween 20 in water and in YESCA medium in the absence of bacteria by surface tensiometry. We first noted that, in the absence of Tween 20, the surface tension of the YESCA medium is lower than that in pure water, which can be attributed to medium components, for example, amino acids and proteins that are surface active and adsorb spontaneously to the air–liquid interface, driven by the removal of nonpolar groups from the bulk solution (Figure 1). In the presence of

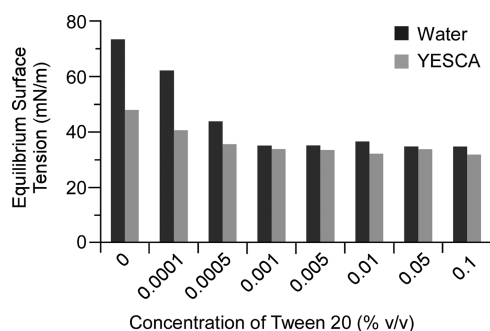


Figure 1. Equilibrium surface tension of Tween 20 in pure water (dark) and in YESCA medium (gray). The transition to a stabilized surface tension occurred at approximately 0.001% Tween 20.

Tween 20, the equilibrium surface tension in both water and YESCA medium decreased, consistent with increased surface adsorption of individual surfactant molecules with increasing concentration (Figure 1). The initial addition of Tween 20 lowered the surface tension in both water and in YESCA medium, and eventually the surface activities in both water and YESCA were similar when the surface tension was dominated by Tween 20.

Influence of Tween 20 on Bacterial Growth. Previous studies have demonstrated that Tween 20 did not significantly inhibit growth of a certain strain of *E. coli*, ATCC 11303, at concentrations up to 2% Tween 20, and that the *E. coli* did not hydrolyze the surfactant.³⁸ We examined the growth of our *E. coli* strain, UTI89, in YESCA nutrient medium as a function of Tween 20 concentration. Over a period of 12 h following inoculation, UTI89 growth was identical among all conditions, and growth curves bifurcated at later hours (Figure 2). Cell cultures grown in the presence of 0.1% and 1% Tween 20 did not reach as high a maximum optical density as the untreated and sub-0.1% Tween-20-treated cultures did. Thus, growth was slightly impaired at Tween 20 concentrations at and above 0.1%. In our subsequent studies on biofilm formation, we

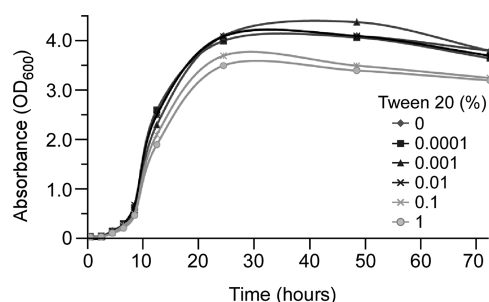


Figure 2. Growth curves of UTI89 in YESCA medium in the absence and presence of increasing Tween 20 concentrations from 0.0001% to 1%. Tween 20 does not influence bacterial viability at concentrations less than or equal to 0.01% and has a minor impact on viability at 0.1 and 1.0% Tween 20.

restricted our use of Tween 20 to concentrations below 0.1% where bacterial growth is not impaired.

Influence of Tween 20 on Macroscopic and Long-Time Biofilm Formation. We examined the potential of Tween 20 to inhibit the long-time UTI89 pellicle formation and UTI89 biofilm formation attached to PVC. Biofilm attached to plastic, growing at the solid–liquid interface, is routinely compared and quantified by a relatively high-throughput method which relies on the ability of the dye crystal violet to indiscriminately bind to biomass.³⁶ Thus, after bacterial growth in wells of a 96-well microtiter plate and after the removal of loosely attached cells by several washes, wells are incubated with a crystal violet solution. After washing and removing unbound crystal violet, the attached crystal violet is solubilized in ethanol and its absorbance at 595 nm is measured to permit quantitative comparisons of biofilm formation among multiple samples. Biofilm attached to plastic decreased slightly at Tween 20 concentrations at or below 0.001% (Figure 3a). Detectable biofilm decreased precipitously at Tween 20 concentrations above 0.001%.

The comparative panel of pellicles, formed at the air–liquid interface in the absence and presence of Tween 20 exhibited a similar concentration-dependent profile upon visual inspection after 5 days of bacterial growth under pellicle-forming conditions, growing static in YESCA medium at 26 °C. Pellicles formed in the presence of 0.0001 and 0.0005% Tween 20 appeared homogeneously opaque and were indistinguishable from the untreated pellicle, while notable variations in the pellicle appearance were observed at and above 0.001% Tween 20 (Figure 3b). At 0.001% Tween 20, a mostly opaque surface eventually formed, but was interrupted by stretched, open pores dispersed over the entire surface area. The patchy appearance of these pores indicates local disconnections in the network of bacterial aggregates that comprise the pellicle. At 0.005% Tween 20, only a small patch of pellicle was eventually observed at the surface and in the center of the well, and was also interrupted by small pores; the rest of the surface appeared clear and liquidlike with no observable film. At 0.01% Tween 20, the entire surface was clear with no visual evidence of the filmlike morphology associated with a pellicle.

Analysis of Pellicle Formation by Interfacial Rheometry. We recently examined the time dependent progression of UTI89 pellicle formation using Brewster-angle microscopy and measurements of the surface elasticity (G_s') and identified distinct stages that accompany bacterial growth in the bulk medium followed by film formation at the surface that is

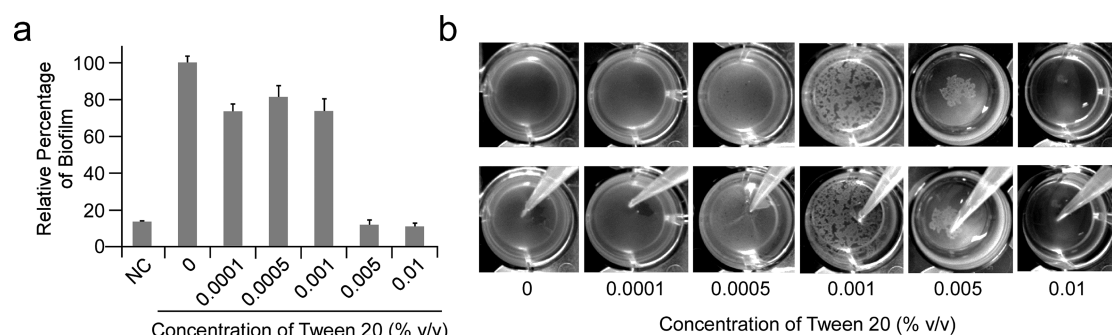


Figure 3. Conventional biofilm assays to assess biofilm formation at the solid–liquid and air–liquid interface. (a) The crystal-violet binding assay compares biofilm formation at the solid–liquid interface using a 96-well microtiter plate format. All biomass attached to the plastic after washing is quantified by staining with crystal violet, dissolution of the dye in ethanol, and quantification by absorbance measurements at 595 nm. Biofilm formation is decreased as the Tween 20 concentration is increased, assayed at 60 h postinoculation. The negative control (NC), UTI89 Δ csgA, does not form an appreciable biofilm. (b) The macroscopic influence of Tween 20 on pellicle formation was examined by visual inspection after 5 days of incubation of bacteria in YESCA broth in a 24-well plate at 26 °C. To aid in visualization of the formed films, photos were taken before⁴⁰ and after (bottom) minor perturbation with a pipet tip. Disruption of the opaque film reveals the translucent underlying nutrient broth. Increasing concentrations of Tween 20 inhibit pellicle formation in a dose-dependent manner.

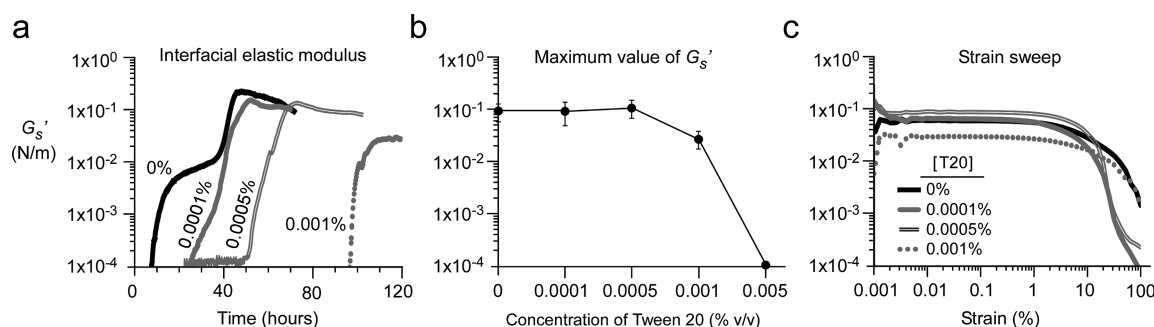


Figure 4. Measurements of the interfacial elastic modulus (G_s') during pellicle formation. (a) Evolution of G_s' during pellicle formation in untreated and Tween-20-treated conditions. (b) Comparison of the highest G_s' values in the untreated and Tween-20 treated conditions. Error bars correspond to the standard error for experiments performed in triplicate. (c) Response of G_s' in the strain sweep from 0 to 100% in untreated and Tween-20-treated conditions.

mediated by curli amyloid fibers.¹⁸ In addition, we observed enhanced surface elasticity of the pellicle and resilience of the pellicle in the presence of shear stress among pellicles with increased curli production, thus correlating molecular composition with mechanical properties.¹⁸ As also demonstrated in this previous work, interfacial viscoelasticity measurements are sensitive to the inception of biofilm formation and measurable signals are produced well in advance of when visual inspection of the interface reveals the presence of a film. Thus, to quantitatively describe the evolution of the surface morphology of pellicles formed in the presence of Tween 20, we examined the evolution of the surface viscoelasticity of the potential pellicle-forming bacterial cultures and measured the interfacial elastic modulus (G_s') as a function of time.

In the untreated sample, the first rise and plateau in G_s' from 10 to 20 h is attributed to bacterial growth as the cells rapidly divide, populating the bulk phase and the surface. Experiments with the curli mutant, UTI89 Δ csgA, demonstrated that this first rise and plateau due to cell growth is curli-independent.¹⁸ This is not surprising since curli expression is upregulated at later times, as cells enter stationary phase. Consistent with the above long-time biofilm results, the pellicles formed in the presence of up to 0.0005% Tween 20 reached a similar plateau and maximum G_s' value, although a detectable lag phase was detected in successively higher Tween 20 concentration regimes (Figure 4a). The disappearance of the first rise-and-

plateau stage in the Tween-20-treated conditions indicates that the bacteria, although able to grow in the bulk phase (as supported also by the growth experiments, Figure 1), are not able to significantly populate the surface as they grow exponentially. Starting at 30 h and at 50 h for the 0.0001% and 0.0005% Tween-20 treated samples, respectively, the G_s' measurements exhibited a single rise that reached the maximum G_s' value, ~ 0.01 N/m, associated with pellicle formation in the absence of Tween 20. Thus, although pellicle formation was delayed, a viscoelastic surface was ultimately produced.

At concentrations at and above 0.001% Tween 20, a diminution of the maximum achievable modulus was observed, along with a significant postponement in the inception of pellicle production (Figure 4a and b). The reduction in the maximum value of the surface elastic modulus under this condition is also attributed to the local disconnectivity of the bacterial pellicle. When the surfactant concentration reaches and exceeds 0.005%, G_s' is reduced to zero (Figure 4b). The samples remained purely viscous and no elastic modulus was detected during the 3–5 day measurements. This percentage corresponds well to the estimated critical micelle concentration (CMC) of Tween 20, reported as 0.006%.³⁹

The tenacities of the pellicles were assessed by shearing the surfaces using a strain sweep from 0% to 100%. As the results presented in Figure 4c suggest, all the pellicles broke down at strains on the order of 10%. The pellicle formed in the

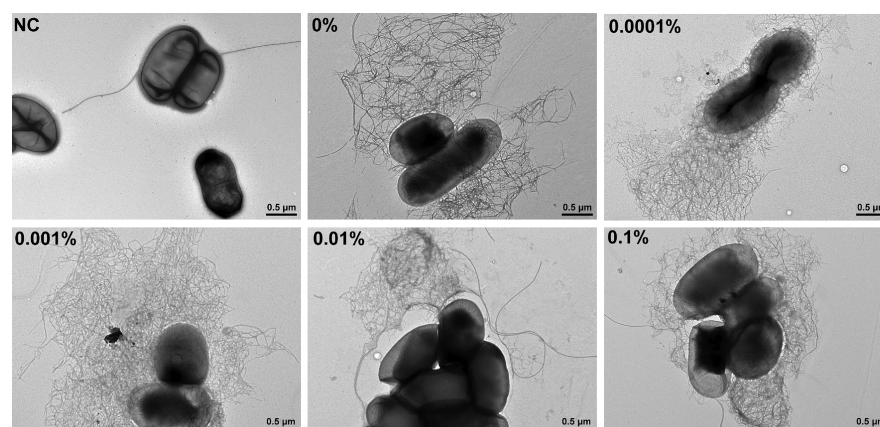


Figure 5. TEM images of UTI89 bacteria grown in the absence and presence of Tween 20 for 48 h. Electron micrographs of untreated UTI89 and cells grown in the presence of 0.0001%, 0.001%, 0.01%, and 0.1% Tween 20 appear similar. Thus, Tween 20 does not appear to influence cellular morphology or curli production. UTI89 Δ csgA does not produce curli and is included as the negative control (NC).

untreated condition was the most robust and sustained the highest strain. The tenacities of pellicles formed in Tween-20-treated conditions below 0.001% were weaker than those in the untreated conditions, characterized by lower breakdown strains and more precipitous diminutions in G_s' when subjected to deformation. The surface of 0.001% Tween-20-treated condition was not deformed as significantly (Figure 4c) and is consistent with the observation that the patches of pellicle were already locally disconnected (Figure 3b).

Cellular and Molecular Phenotypes. The above experiments demonstrate that Tween 20 inhibits curli-dependent biofilm formation in UTI89 without inhibiting cell viability. Thus, we sought to determine whether the surfactant could, alternatively, be preventing curli assembly in *E. coli* and thus preventing curli-dependent biofilm formation. Similar to the growth curve determinations in Figure 2, we grew bacteria in the presence and absence of Tween 20 in YESCA nutrient medium at 26 °C and employed TEM to visualize the bacteria and assess whether there could be morphological changes to cells grown in the presence of Tween 20 and whether there is any obvious alteration of curli production. There was no appreciable difference in cell morphology between the untreated and treated conditions (Figure 5). There were also no obvious detectable differences in curli production observed in the TEM micrographs of bacteria grown in the presence of increasing concentrations of Tween 20 (Figure 5). Furthermore, curli production was quantified by Western blot analysis. For these assays, harvested whole-cell samples were prepared as cell pellets corresponding to 1 mL an OD₆₀₀ 1.0 culture. Each cell pellet was treated with HFIP to dissociate CsgA monomers from the amyloid fiber. HFIP was removed by vacuum centrifugation, and samples were resuspended in SDS-PAGE loading buffer for Western blot analysis. Curli production was similar among untreated and treated conditions (Figure 6). No CsgA was detected in the absence of HFIP treatment, indicating that all the CsgA was in amyloid form, requiring HFIP for dissolution, which is typical for curli fibers (data not shown).^{4,9} Together, the EM and Western blot results demonstrate that, at the molecular level, Tween 20 is not inhibiting curli production. Therefore, our results suggest that Tween 20 could be inhibiting pellicle formation through a physical influence, altering the properties of the air–liquid interface and preventing enhanced colonization and pellicle formation at this interface.

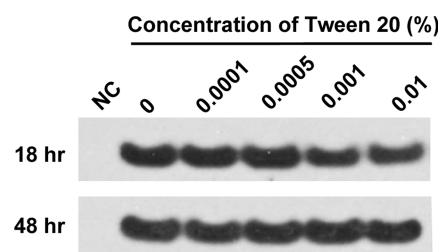


Figure 6. Western blot analysis of CsgA production after 18 and 48 h of cell growth. According to standard curli protein quantification protocols, harvested whole-cell samples were prepared as cell pellets corresponding to 1 mL cell culture with an OD₆₀₀ of 1.0. Each cell pellet was treated with hexafluoroisopropanol (HFIP) to dissociate CsgA monomers from the amyloid fiber. HFIP was removed by vacuum centrifugation, and samples were resuspended in SDS-PAGE loading buffer for Western blot analysis. CsgA production is similar among untreated and Tween 20 treated cells. UTI89 Δ csgA does not produce curli and is included as the negative control (NC).

CONCLUSIONS

We report for the first time the discovery that Tween 20 prevents biofilm formation at the air–liquid interface by uropathogenic *E. coli*, and we compare in detail the morphological, biochemical, and viscoelastic properties of untreated and surfactant-treated biofilms. Tween 20 does not impede growth or inhibit curli production at concentrations less than or equal to 0.01%. Thus, at the molecular level, there is no obvious physiological response to the presence of Tween 20. The inhibition of pellicle formation and the observed interfacial rheological measurements suggest that Tween 20, which exhibits an increased tendency to persist as micelles near and above the CMC, accumulates at the air–liquid interface, competing with cells for surface adsorption, and prevents the cells from coupling mechanically at the interface. Our results support a model in which the hydrophobic curli fibers require the air–liquid interface to form strong physical entanglements and to form a network that can support shear stress. In this model, Tween 20 physically occludes the surface, preventing the formation of a curli-mediated bacterial network at the air–liquid interface.

The complex interaction of polysorbate surfactants and proteins and surfaces is an important subject for biological, chemical, pharmaceutical, and food processing industries. In

addition, the role and the structure and function of amyloid-integrated biofilms is a burgeoning area of research investigation since the discovery of curli as an amyloid fiber in 2002. Both *E. coli* and *Salmonella* produce curli fibers, and we have demonstrated the ability of Tween 20 to inhibit amyloid-dependent biofilm formation by the uropathogenic *E. coli* strain, UTI89. *E. coli* strains vary widely in their ability to produce other adhesive fibers, proteins, and small molecules. As described earlier, other bacteria such as *B. subtilis* can even exhibit enhanced pellicle formation in the presence of a surfactant. Thus, future work with different curli-producing *E. coli* strains and other pellicle-forming microorganisms will be of value. The physico-biological approach we applied in this study can be readily extended to other surfactants and small molecules and to other microorganisms. Furthermore, our discovery that Tween 20 can prevent biofilm formation even though curli are still produced highlights the ability to prevent cellular aggregation and biofilm formation even after biofilm components are made.

AUTHOR INFORMATION

Corresponding Author

*E-mail: ggf@stanford.edu (G.G.F.); cegelski@stanford.edu (L.C.).

Author Contributions

[§]These authors contributed equally to this work.

Notes

The authors declare no competing financial interest.

ACKNOWLEDGMENTS

G.G.F. acknowledges support from the CBET Division of NSF. L.C. acknowledges support from the NIH Director's New Innovator Award (1DP2OD007488), Stanford University, and the Stanford Terman Fellowship. L.C. holds a Career Award at the Scientific Interface from the Burroughs Wellcome Fund.

REFERENCES

- (1) Costerton, J. W.; Cheng, K. J.; Geesey, G. G.; Ladd, T. I.; Nickel, J. C.; Dasgupta, M.; Marrie, T. J. Bacterial Biofilms in Nature and Disease. *Annu. Rev. Microbiol.* **1987**, *41*, 435–464.
- (2) Costerton, J. W.; Lewandowski, Z.; Caldwell, D. E.; Korber, D. R.; Lappinscott, H. M. Microbial Biofilms. *Annu. Rev. Microbiol.* **1995**, *49*, 711–745.
- (3) Flemming, H. C. Biofouling in water systems - cases, causes and countermeasures. *Appl. Microbiol. Biotechnol.* **2002**, *59*, 629–640.
- (4) Lim, J. Y.; May, J. M.; Cegelski, L. Dimethyl sulfoxide and ethanol elicit increased amyloid biogenesis and amyloid-integrated biofilm formation in *Escherichia coli*. *Appl. Environ. Microbiol.* **2012**, *78*, 3369–78.
- (5) Boyer, R. R.; Sumner, S. S.; Williams, R. C.; Pierson, M. D.; Popham, D. L.; Kniel, K. E. Influence of curli expression by *Escherichia coli* O157:H7 on the cell's overall hydrophobicity, charge, and ability to attach to lettuce. *J. Food Prot.* **2007**, *70*, 1339–45.
- (6) Pawar, D. M.; Rossman, M. L.; Chen, J. Role of curli fimbriae in mediating the cells of enterohaemorrhagic *Escherichia coli* to attach to abiotic surfaces. *J. Appl. Microbiol.* **2005**, *99*, 418–25.
- (7) Ryu, J. H.; Beuchat, L. R. Biofilm formation by *Escherichia coli* O157:H7 on stainless steel: effect of exopolysaccharide and Curli production on its resistance to chlorine. *Appl. Environ. Microbiol.* **2005**, *71*, 247–54.
- (8) Barnhart, M. M.; Chapman, M. R. Curli biogenesis and function. *Annu. Rev. Microbiol.* **2006**, *60*, 131–47.
- (9) Chapman, M. R.; Robinson, L. S.; Pinkner, J. S.; Roth, R.; Heuser, J.; Hammar, M.; Normark, S.; Hultgren, S. J. Role of *Escherichia coli*

curli operons in directing amyloid fiber formation. *Science* **2002**, *295*, 851–855.

(10) Hammar, M.; Bian, Z.; Normark, S. Nucleator-dependent intercellular assembly of adhesive curli organelles in *Escherichia coli*. *Proc. Natl. Acad. Sci. U.S.A.* **1996**, *93*, 6562–6566.

(11) Robinson, L. S.; Ashman, E. M.; Hultgren, S. J.; Chapman, M. R. Secretion of curli fibre subunits is mediated by the outer membrane-localized CsgG protein. *Mol. Microbiol.* **2006**, *59*, 870–881.

(12) Nenninger, A. A.; Robinson, L. S.; Hultgren, S. J. Localized and efficient curli nucleation requires the chaperone-like amyloid assembly protein CsgF. *Proc. Natl. Acad. Sci. U.S.A.* **2009**, *106*, 900–905.

(13) Alteri, C. J.; Xicohtencatl-Cortes, J.; Hess, S.; Caballero-Olin, G.; Giron, J. A.; Friedman, R. L. *Mycobacterium tuberculosis* produces pili during human infection. *Proc. Natl. Acad. Sci. U.S.A.* **2007**, *104*, 5145–5150.

(14) Capstick, D. S.; Jomaa, A.; Hanke, C.; Ortega, J.; Elliot, M. A. Dual amyloid domains promote differential functioning of the chaplin proteins during *Streptomyces aerial* morphogenesis. *Proc. Natl. Acad. Sci. U.S.A.* **2011**, *108*, 9821–9826.

(15) Dueholm, M. S.; Petersen, S. V.; Sonderkaer, M.; Larsen, P.; Christiansen, G.; Hein, K. L.; Enghild, J. J.; Nielsen, J. L.; Nielsen, K. L.; Nielsen, P. H.; Otzen, D. E. Functional amyloid in *Pseudomonas*. *Mol. Microbiol.* **2010**, *77*, 1009–1020.

(16) Romero, D.; Aguilar, C.; Losick, R.; Kolter, R. Amyloid fibers provide structural integrity to *Bacillus subtilis* biofilms. *Proc. Natl. Acad. Sci. U.S.A.* **2010**, *107*, 2230–2234.

(17) Cogan, T. A.; Jorgensen, F.; Lappin-Scott, H. M.; Benson, C. E.; Woodward, M. J.; Humphrey, T. J. Flagella and curli fimbriae are important for the growth of *Salmonella enterica* serovars in hen eggs. *Microbiology* **2004**, *150*, 1063–1071.

(18) Wu, C.; Lim, J. Y.; Fuller, G. G.; Cegelski, L. Quantitative Analysis of Amyloid-Integrated Biofilms Formed by Uropathogenic *Escherichia coli* at the Air-Liquid Interface. *Biophys. J.* **2012**, *103*, 464–471.

(19) Hoffmann, C.; Blume, A.; Miller, I.; Garidel, P. Insights into protein-polysorbate interactions analysed by means of isothermal titration and differential scanning calorimetry. *Eur. Biophys. J.* **2009**, *38*, 557–568.

(20) Kerwin, B. A. Polysorbates 20 and 80 used in the formulation of protein biotherapeutics: Structure and degradation pathways. *J. Pharm. Sci.* **2008**, *97*, 2924–2935.

(21) Lam, X. M.; Yang, J. Y.; Cleland, J. L. Antioxidants for prevention of methionine oxidation in recombinant monoclonal antibody HER2. *J. Pharm. Sci.* **1997**, *86*, 1250–1255.

(22) Mahler, H. C.; Senner, F.; Maeder, K.; Mueller, R. Surface Activity of a Monoclonal Antibody. *J. Pharm. Sci.* **2009**, *98*, 4525–4533.

(23) Patapoff, T. W.; Esue, O. Polysorbate 20 prevents the precipitation of a monoclonal antibody during shear. *Pharm. Dev. Technol.* **2009**, *14*, 659–64.

(24) Boyd, J.; Parkinson, C.; Sherman, P. Factors affecting emulsion stability, and the HLB concept. *J. Colloid Interface Sci.* **1972**, *41*, 359–370.

(25) Dalgleish, D. G.; Srinivasan, M.; Singh, H. Surface-Properties of Oil-in-Water Emulsion Droplets Containing Casein and Tween-60. *J. Agric. Food. Chem.* **1995**, *43*, 2351–2355.

(26) Dickinson, E.; Ritzoulis, C. Creaming and rheology of oil-in-water emulsions containing sodium dodecyl sulfate and sodium caseinate. *J. Colloid Interface Sci.* **2000**, *224*, 148–154.

(27) Dimitrova, T. D.; Leal-Calderon, F. Forces between emulsion droplets stabilized with Tween 20 and proteins. *Langmuir* **1999**, *15*, 8813–8821.

(28) Nino, R. R.; Patino, J. M. R. Surface tension of bovine serum albumin and tween 20 at the air-aqueous interface. *J. Am. Oil Chem. Soc.* **1998**, *75*, 1241–1248.

(29) Toutain-Kidd, C. M.; Kadivar, S. C.; Bramante, C. T.; Bobin, S. A.; Zegans, M. E. Polysorbate 80 Inhibition of *Pseudomonas aeruginosa* Biofilm Formation and Its Cleavage by the Secreted Lipase LipA. *Antimicrob. Agents Chemother.* **2009**, *53*, 136–145.

- (30) Mireles, J. R.; Toguchi, A.; Harshey, R. M. *Salmonella enterica* serovar typhimurium swarming mutants with altered biofilm-forming abilities: Surfactin inhibits biofilm formation. *J. Bacteriol.* **2001**, *183*, 5848–5854.
- (31) Wang, R.; Khan, B. A.; Cheung, G. Y. C.; Bach, T. H. L.; Jameson-Lee, M.; Kong, K. F.; Queck, S. Y.; Otto, M. *Staphylococcus epidermidis* surfactant peptides promote biofilm maturation and dissemination of biofilm-associated infection in mice. *J. Clin. Invest.* **2011**, *121*, 238–248.
- (32) Straight, P. D.; Willey, J. M.; Kolter, R. Interactions between *Streptomyces coelicolor* and *Bacillus subtilis*: Role of surfactants in raising aerial structures. *J. Bacteriol.* **2006**, *188*, 4918–4925.
- (33) Lopez, D.; Fischbach, M. A.; Chu, F.; Losick, R.; Kolter, R. Structurally diverse natural products that cause potassium leakage trigger multicellularity in *Bacillus subtilis*. *Proc. Natl. Acad. Sci. U.S.A.* **2009**, *106*, 280–285.
- (34) Hoben, H. J.; Somasegaran, P. Comparison of the Pour, Spread, and Drop Plate Methods for Enumeration of Rhizobium spp. in Inoculants Made from Presterilized Peat. *Appl. Environ. Microbiol.* **1982**, *44*, 1246–7.
- (35) Shchukin, E. D.; pertov, A. V.; Amelina, E. A.; Zelenev, A. S. *Colloid and Surface Chemistry, Studies in interface science*; Elsevier Science: Oxford, U.K., 2002; Vol. 12.
- (36) O'Toole, G. A.; Kolter, R. Initiation of biofilm formation in *Pseudomonas fluorescens* WCS365 proceeds via multiple, convergent signalling pathways: a genetic analysis. *Mol. Microbiol.* **1998**, *28*, 449–461.
- (37) Nenninger, A. A.; Robinson, L. S.; Hammer, N. D.; Epstein, E. A.; Badtke, M. P.; Hultgren, S. J.; Chapman, M. R. CsgE is a curli secretion specificity factor that prevents amyloid fibre aggregation. *Mol. Microbiol.* **2011**, *81*, 486–499.
- (38) Rose, M. J.; Aron, S. A.; Janicki, B. W. Effect of Various Nonionic Surfactants on Growth of *Escherichia Coli*. *J. Bacteriol.* **1966**, *91*, 1863.
- (39) Helenius, A.; McCaslin, D. R.; Fries, E.; Tanford, C. Properties of Detergents. *Methods Enzymol.* **1979**, 734–749.
- (40) Capstick, T. G. D.; Laycock, D.; Lipman, M. C. I.; TB, U. C. S. Treatment interruptions and inconsistent supply of anti-tuberculosis drugs in the United Kingdom. *Int. J. Tuberc. Lung Dis.* **2011**, *15*, 754–760.